Rayleigh-Taylor and Kelvin-Helmholtz Instabilities in Targets Accelerated by Laser Ablation

Mark H. Emery, John H. Gardner, and Jay P. Boris
Laboratory for Computational Physics, Naval Research Laboratory, Washington, D.C. 20375
(Received 20 July 1981)

With use of the FAST2D laser-shell model, the acceleration of a 20-μm-thick plastic foil up to 160 km/s has been simulated. It is possible to follow the Rayleigh-Taylor bubble-and-spike development far into the nonlinear regime and beyond the point of foil fragmentation. Strong shear flow develops which evolves into the Kelvin-Helmholtz instability. The Kelvin-Helmholtz instability causes the tips of the spikes to widen and as a result reduce their rate of "fall."

PACS numbers: 52.65.+z, 52.35.Py, 52.50.Jm

The Rayleigh-Taylor (RT)[1] instability arises in the acceleration of a fluid by one of lower density. This instability may represent an obstacle to inertial-confinement fusion by destroying the spherical symmetry of high-aspect-ratio imploding shells. The RT instability causes corrugations on the ablation layer between the cold, high-density shell and the hot, low-density ablated material. These corrugations eventually grow nonlinearly to form the typical bubble-and-spike[2] structure. In addition the shear flow that develops as the bubble-and-spike structure evolves can lead to the Kelvin-Helmholtz (KH)[3,4] instability.

We report here on our investigation of the RT and KH instabilities in laser ablatively accelerated flat targets using the FAST2D laser-shell simulation code.[5,6] This is a fully two-dimensional Cartesian code with a sliding Eulerian grid with variable grid spacing. The grid spacing is 0.25 μm for ten zones on either side of the ablation layer and increases uniformly to a 2-μm spacing for most of the rest of the grid. The finely zoned region near the ablation layer is required in order to resolve accurately the steep density gradient. The refined subzoning follows the ablation front throughout the course of the run. The zones in the underdense plasma beyond the critical surface and in the low-density rear portion of the foil are stretched. The system has 40 zones transverse to the laser beam (y direction) and 120 zones parallel (x direction). The system is periodic in the transverse direction.

FAST2D solves the ideal hydrodynamic equations using the flux-corrected transport (FCT)[7] algorithms with a two-dimensional classical ($T^{5/2}$) plasma thermal conduction routine. The initial density, pressure, and temperature profiles for a 20-μm-thick, plastic (CH) foil irradiated with an absorbed laser intensity of 1.0×10^{13} W/cm^2 (1.05 μm) are generated from a one-dimensional, analytic, quasistatic equilibrium model.[8] The analytic solutions have been shown to have provided an adequate steady state when FAST2D is run in a one-dimensional mode,[9] i.e., *sans* perturbation. There are only minor changes in the profiles [0 (0.5%) change in the density gradient] after 1000 time steps (~3 ns). FAST2D also compares well with Naval Research Laboratory experimental data on hydrodynamic efficiencies, ablation pressures, and target velocities[9] and with fluid blowoff profiles.[10]

The initial perturbation is obtained by perturbing the density profile at its peak. The first ten modes are excited with equal amplitudes and random phases corresponding to a total initial density perturbation of 8% $[(\rho_{\max}-\rho_{\min})/\langle\rho\rangle = 0.08)$. The longest wavelength excited is 100 μm.

The growth rates for the first five modes are compared with the classical value, $\gamma_c=(kg)^{1/2}$, in Fig. 1. These growth rates are well below the classical value, in agreement with other time-dependent calculations.[11]

Figure 2 shows a time sequence of density contours when the system is far into the nonlinear regime. By 8 ns the bubble-and-spike structure is quite prominent. The spikes grow rapidly in amplitude and the classical tip spreading is well developed at the shoulders of the spikes by 9.2 ns. As the spikes accelerate, lateral flow continues to widen the tips until the foil fragments at 10.6 ns.

The tip spreading is due to the nonlinear wrap-up phase of the Kelvin-Helmholtz instability in the shear layer at the interface between the falling spike and the rising bubble. That a very strong shear layer develops between the bubble and the spike is evident in the vector fluid velocity field (Fig. 3) spanning the region between the

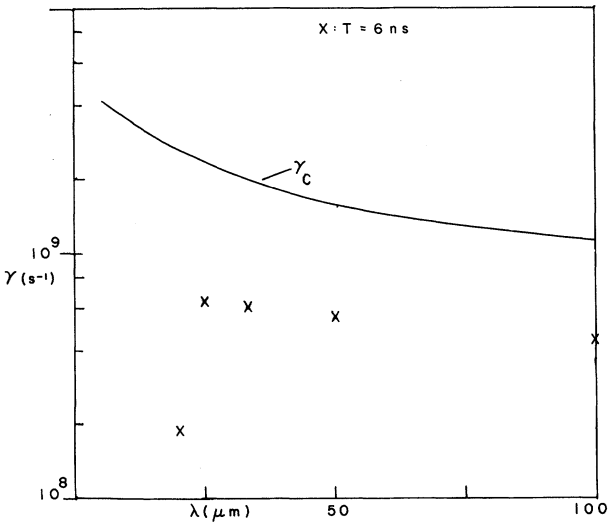

FIG. 1. A comparison of the growth rates of the first five modes with the classical value $\gamma_c = (kg)^{1/2}$.

arrows on the density contour plots of Fig. 2. The lateral flow that causes the tip widening is clearly apparent in the velocity plots. The solid line is the 10% density contour. Note that the shear flow and the strong circulatory flow (vortex flow) develops on the high-density side of the

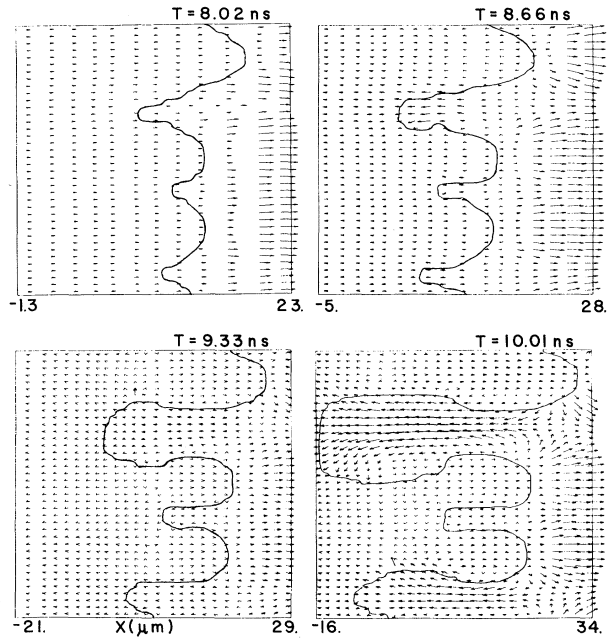

FIG. 3. Vector fluid velocity plots for the region spanned by the vertical arrows of Fig. 2. The solid line is the 10% density contour. Note the vortices developing at the bubble-spike interface at 9.2 and 10 ns.

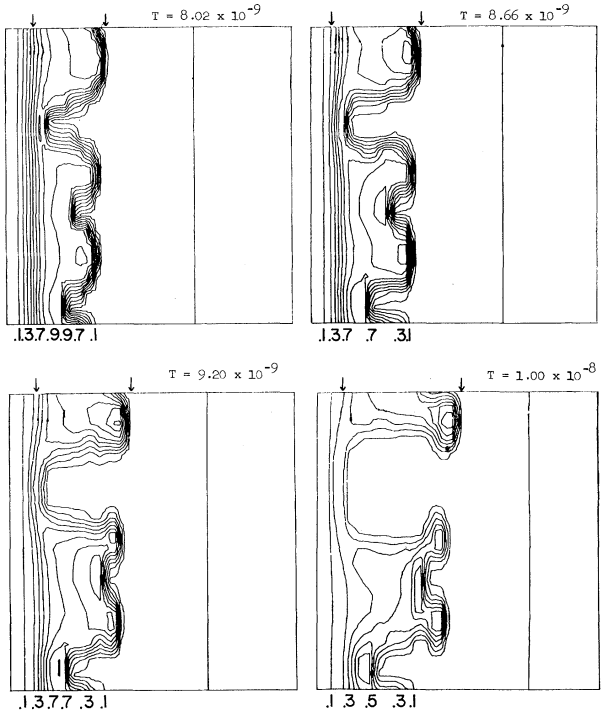

FIG. 2. Density contours at different times showing the development the bubble-and-spike formation and the subsequent tip spreading. The lines are contours of constant density in 10% increments of the maximum density (ρ_{max} = 0.71 g/cm^3) counting from the outside inward. The right-most contour is the critical surface.

contour. The vortices are typically entrained between the 10% and 30% contours giving an Atwood number of 0.5, within the range for the

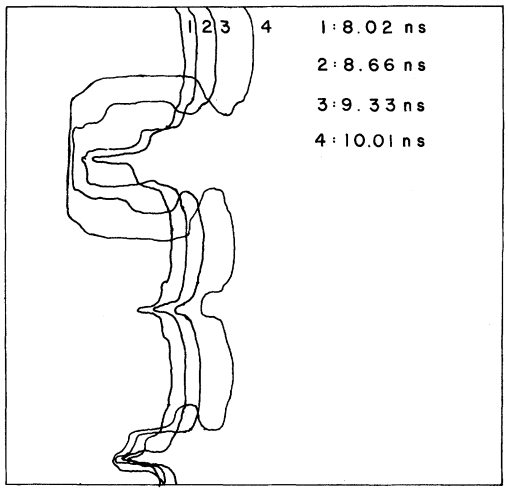

FIG. 4. Bubble-and-spike contours at various times. Note the large increase in the area of the bubble between 9.33 and 10.01 ns.

KH instability.[3,4,12] The lack of a strong spiral rollup in the wake of the bulge[3,12] is due to the density gradient and mass ablation effects; however, the lateral growth of the spike tips, the vortices at the spike shoulders, and the flattening of the rear edge of the spike (due to the reverse flow set up by the vortices) are all definitive signatures of the KH instability.

The time evolution of the bubble-and-spike formation is shown in Fig. 4. Up to about 10 ns the growth of the spike outpaces that of the bubble. Initially the spike experiences less drag than the bubble since the "heavy" spike is replacing fluid with a smaller density whereas the "light" bubble is attempting to rise through a denser medium. It is not until the area of the bubble becomes quite large, thereby increasing its buoyancy, that the bubble velocity approaches the spike velocity.

The amplitude of the bubble-and-spike formation (ΔX_{bs}) is plotted as a function of time in Fig. 5. Here we have also plotted the distance from the critical surface to the spike tip (ΔX_{cs}) and the distance from the rear of the foil to the bubble (ΔX_{rb})—a measure of how far the bubble has "risen." The spike "falls" nearly exponentially up to saturation at about 10 ns. Note the reduction in the spike growth rate after 8 ns. It is at about this time that the tip widening appears. The bubble "rise" is much slower and approaches zero between 9 and 10 ns. During this period the area of the bubble is increasing radically (see Fig. 4) until the bubble buoyancy is large enough, coupled with the reduced mass of the shell due to ablation, that the bubble bursts through the rear of the foil.

The temperature contours, Fig. 6, indicate a strong temperature gradient at the spike tip, corresponding to a large mass-ablation rate there, albeit, not large enough to cause a recession of the spike growth.[11] Note that the temperature of the bubble is quite cold and uniform, and thus mass ablation must be removed from consideration as a possible stabilizing mechanism for the KH instability that appears at the spike-bubble interface.

The KH instability is, in fact, the stabilizing mechanism here. The spike tip widening is due to the growth of the KH instability in the shear layer at the bubble-and-spike interface. This tip widening increases the frontal area of the spike, thereby increasing its drag and reducing its rate of "fall." With a thicker shell and for short-wavelength perturbations the spike tips

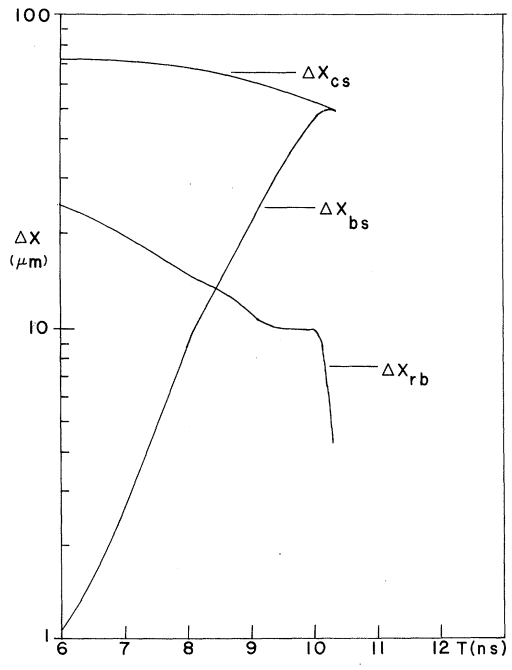

FIG. 5. A plot of the spike amplitude (ΔX_{bs}), the distance between the critical surface and spike tip (ΔX_{cs}), and the distance between the rear of the foil and the bubble (ΔX_{rb}) as a function of time.

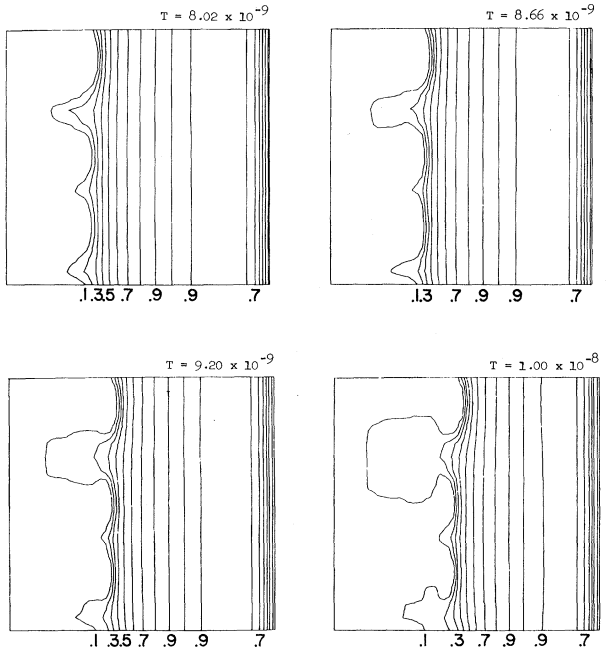

FIG. 6. Temperature contours corresponding to Figs. 2 and 3. The maximum temperature is 700 eV.

may widen enough to seal off the bubble and form a uniform ablation front, thereby saturating the spike growth well before shell fragmentation. This aspect of the problem is now being investigated and is the subject of a future report.

Since the growth rates of the instability are well below the classical values, at 10 ns the rear of the foil is still being accelerated uniformly. At this time the foil velocity is 160 km/s—within the range required for inertial fusion. The foil has been pushed a distance of 800 μm—forty times its original thickness.

The authors gratefully acknowledge the helpful conversations with A. L. Cooper, M. J. Fritts, S. Bodner, J. Grun, M. Herbst, and B. Ripin at the Naval Research Laboratory. We thank M. Fry of Science Applications, Inc. for the use of his vector plotting routine. This research was supported by the U. S. Department of Energy.

[1]Lord Rayleigh, *Theory of Sound* (Dover, New York, 1945), 2nd ed., Vol. 2; G. I. Taylor, Proc. Roy. Soc. (London), Ser. A 201, 192 (1930).

[2]F. H. Harlow and J. E. Welch, Phys. Fluids 9, 842 (1966).

[3]B. J. Daly, Phys. Fluids 10, 297 (1967).

[4]H. Helmholtz, Philos. Mag., Ser. 4, 36, 337 (1868); Lord Kelvin, *Hydrodynamics and General Dynamics* (Cambridge Univ. Press, Cambridge, 1910), pp. 69ff.

[5]J. P. Boris, Comments Plasma Phys. Controlled Fusion 3, 1 (1977).

[6]M. H. Emery, J. H. Orens, J. H. Gardner, and J. P. Boris, Naval Research Laboratory Memo Report 4500, 1981 (to be published), and Bull. Am. Phys. Soc. 25, 947 (1980).

[7]J. P. Boris and D. L. Book, Methods Comput. Phys. 16, 85 (1976).

[8]J. H. Orens, Naval Research Laboratory Memo Report No. 4167, 1980 (unpublished); J. H. Orens *et al.*, Bull. Am. Phys. Soc. 23, 750 (1978).

[9]P. J. Moffa *et al.*, Bull. Am. Phys. Soc. 24, 946 (1976); Naval Research Laboratory Plasma Interaction Group, Naval Research Laboratory Report No. 4369, 1980 (unpublished).

[10]M. Herbst *et al.*, Bull. Am. Phys. Soc. 26, 1024 (1981).

[11]R. L. McCrory *et al.*, Phys. Rev. Lett. 46, 336 (1981).

[12]G. R. Baker *et al.*, Phys. Fluids 23, 1485 (1980).

Catastrophes in the ELMO Bumpy Torus

George Vahala and Alkesh Punjabi
Department of Physics, College of William & Mary, Williamsburg, Virginia 23185

and

Edward G. Harris
Department of Physics, University of Tennessee, Knoxville, Tennessee 37916,[a] *and Oak Ridge National Laboratory, Oak Ridge, Tennessee 37830*

(Received 14 September 1981)

The simple neoclassical nonresonant-point model of Hedrick *et al.* is slightly modified by leaving the ion transport unspecified (since it is now known to be resonant). Small continuous changes in the microwave power/neutral density can cause hysteresis and catastrophe jumps in the equilibria, in qualitative agreement with experiment.

PACS number: 52.55.Gb

In the ELMO bumpy torus (EBT) experiment, a series of toroidally linked mirror machines are stabilized by hot-electron rings which are themselves stabilized by the toroidal core plasma. The usual vertical drifts are now modified by the poloidal ∇B and $\vec{E}\times\vec{B}$ drifts (produced by the bumpiness in the toroidal magnetic field and by the ambipolar radial electric field) yielding particle confinement without the tokamak/stellarator use of a rotation transform.

One of the interesting experimental observations made on EBT is the existence of three different modes of operation as a function of the two normal experimental parameters: p_0 the background pressure, and P_μ, the microwave power delivered to the plasma at the appropriate resonant frequencies necessary for the generation of the hot-electron rings (Fig. 1). For large P_μ (and sufficiently small p_0) one encounters the so-called mirror or M mode in which the plasma behaves

